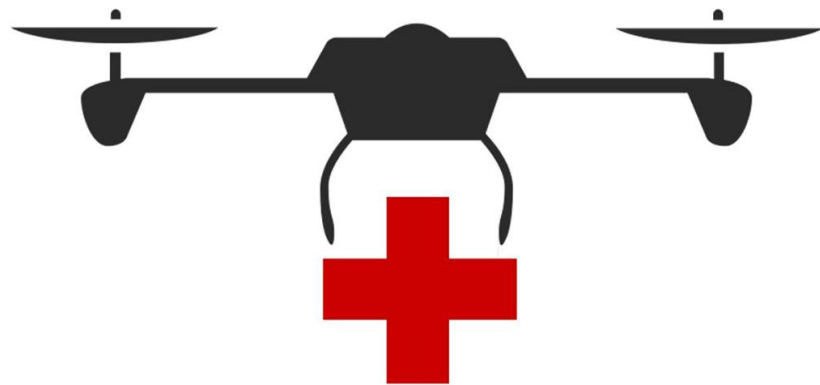


MENG GROUP DESIGN PROJECT 2019



MEDICAIR

Autonomous Drone Delivery

Technical Report - Sensor Group

Student: Łukasz Śliwiński

CID: 01240212

1st Supervisor: Dr Mirko Kovac

2nd Supervisor: Dr Vito L Tagarielli

Date: June 17, 2019

Abstract

Unmanned vehicles serve in an increasing number of real-world applications - from food transportation to military purposes. The task of 2019 ADD Group Design Project was to design and construct an autonomous drone which would be employed in medical services. It would aid in transportation of fragile medical supplies to ambulances sent out for intervention. One of the irreplaceable parts of every unmanned vehicle is a GPS device which enables tracking and state estimation. This specific drone was designed to use Real-Time-Kinematics GPS - a device that offers a centimetre level of accuracy. A series of tests were carried out to evaluate its performance. It was concluded that the high accuracy is obtainable and it would greatly facilitate the drone performance. Due to unexpected circumstances the drone had to use a conventional GPS device for testing but was able to complete simplified flight tasks.

Acknowledgements

I would like to thank my supervisor and personal tutor Dr Mirko Kovac
for guidance throughout this project and my studies.

I would also like to acknowledge PhD student Feng Xiao
for his support, availability and lightning-fast responses to emails.

And lastly, I would like to thank my whole Group Design Project team
for excellent cooperation, perseverance and great team spirit.

Contents

Abstract	i
Acknowledgements	i
Table of Contents	ii
List of Figures	iii
List of Tables	iii
1 Introduction	1
2 Sensor team	1
2.1 Literature Review	1
2.2 Constraints and Trade-offs	1
2.3 Final choice	2
3 GPS Navigation overview	2
4 Here+ RTK GPS	3
4.1 Manufacturer specification and usage	3
4.2 Mounting the rover on the drone and positioning the base module	4
4.3 Accuracy tests	5
4.4 Discussion	6
4.4.1 Static test accuracy	6
4.4.2 /global vs /raw/fix	6
4.4.3 Frequency analysis	7
4.4.4 Circle tests	9
4.5 Improving GPS performance with HxGN SmartNet	9
5 RTK GPS failure	10
5.1 Substitution evaluation	10
5.1.1 Manual base coordinates setup	10
5.1.2 RTK GPS Reach	10
6 Final solution	10
6.1 New accuracy discussion	11
6.2 Performance at Silwood testing site (Figure 28)	12
7 Conclusions	12
A Appendix	15

List of Figures

1	Mission Profile with annotated sensor team challenges	1
2	Final sensor configuration	2
3	GPS Navigation system schematic	3
4	Survey-in status info in QGC (left); RTK GPS streaming status info in QGC (right)	3
5	Base module	3
6	GPS rover module	3
7	Rover - PixHawk wiring schematic used	4
8	Tripod with base module mounted on top	4
9	Drone with GPS rover mounted on the mast	4
10	/raw/fix GPS position in ENU frame of reference over time for the base accuracy 6 m	5
11	/global GPS position in ENU frame of reference over time for the base accuracy 6 m	5
12	/raw/fix GPS position in ENU frame of reference over time for the base accuracy 2 m	6
13	/global GPS position in ENU frame of reference over time for the base accuracy 2 m	6
14	/global GPS data from circle tests with the base accuracy 2 m (left) and 6 m (right)	6
15	Single-sided amplitude spectrum of GPS coordinates in ENU frame of reference for the base accuracy 6 m for low frequencies $\in (0.0, 0.1)$ Hz	7
16	Single-sided amplitude spectrum of GPS coordinates in ENU frame of reference for the base accuracy 6 m for high frequencies $\in (0.1, 4.0)$ Hz	7
17	Single-sided amplitude spectrum of GPS coordinates in ENU frame of reference for the base accuracy 6 m for low frequencies $\in (0.0, 0.1)$ Hz	7
18	Single-sided amplitude spectrum of GPS coordinates in ENU frame of reference for the base accuracy 2 m for high frequencies $\in (0.1, 4.0)$ Hz	7
19	Circle test GPS position in ENU frame of reference over time for the base accuracy of 6 m	8
20	Circle test GPS position in ENU frame of reference over time for the base accuracy of 2 m	8
21	Radius error distribution for base accuracy 6 m	9
22	Radius error distribution for base accuracy 2 m	9
23	HxGN SmartNet base station (adapted from [1])	9
24	Base module cable end (left) and the survey-in status information indicating the problem (right)	10
25	/raw/fix GPS position in ENU frame of reference over time for the rover without the base corrections	11
26	Single-sided amplitude spectrum of GPS coor-dinates in ENU frame of reference for the rover without base corrections for low frequencies $\in (0.0, 0.1)$ Hz	11
27	Single-sided amplitude spectrum of GPS coordinates in ENU frame of reference for the rover without base corrections for high frequencies $\in (0.1, 4)$ Hz	11
28	Testing site at Silwood	12

List of Tables

1	Matrix showing trade-off connected to choosing sensor configuration	2
2	GPS results from static tests (Phone data was obtained using same procedure as with RTK GPS data but at different time and location)	8
3	GPS results from circle tests	8
4	GPS results from static test on the rover without the base corrections	11

1 Introduction

The aim of the project was to create an autonomous drone capable of performing a given mission. The project briefing specified that the drone has to pick up a fragile item and deliver it to a given location. Additionally, it had to be able to automatically avoid obstacles found on the way to the delivery point. As the details of the mission profile were not given, the group could decide to add some complexity and modify the mission profile to fit it to a real-world application. After hours of brainstorming and discussion, it was decided that the drone will be employed in medical services. It often happens that after ambulances are sent into the field, they might lack certain supplies. The drone will pick up the fragile supply from a warehouse, track the specified ambulance and finally land on it and deliver the package. It was decided that for testing the fragile supply will be an egg and the ambulance will be represented by an RC car with an attached landing pad.

2 Sensor team

The task of the sensor team was to come up with the sensor configuration and choose the sensor models that will suffice to complete the mission in the best way possible. After examination of the mission profile, specific challenges were identified for the sensor subgroup (see Figure 1). The sensors had to enable the drone to:

- Vision track the object and the landing field.
- Navigate using GPS.
- Detect obstacles.

A literature review was performed to make sure that the decisions were well informed and that the chosen configuration was feasible.

2.1 Literature Review

Paper [2] presents a drone of similar size to ours which was tasked with tracking a moving object using an RGB camera. The marker was a simple sphere. The drone used a single camera and processor with similar processing power. It could achieve speeds up to 5 m/s. A similar vehicle was described in [3]. This one was equipped with a weaker processor, used a smartphone camera and had to land on a moving landing pad. The speed of the landing field was less than 1m/s. Field report [4] presented a drone used for indoor SLAM (Simultaneous Localization and Mapping). It used multiple laser range-finders, two stereo cameras and a colour camera. The sensor input was processed on board using 1.6 GHz Intel Atom-based flight computer. The drone had robust sensing abilities but its speed was up to 1.5 m/s.

2.2 Constraints and Trade-offs

The project had specified hard and soft constraints. The hard constraints were the £500 budget for the project as well as the predefined drone frame and motors. The soft constraints were due to the fact that some of the onboard devices were already given at the start and thus it was inefficient to replace them. These included:

- ODROID computer,
- TeraRanger Tower,
- TeraBee 3D cam,
- HERE+ RTK GPS (Real-Time-Kinematic Global-Positioning-Satellite),
- PX4Flow sensor,
- battery.

Predefined batteries and motors constrained the total mass of the drone. Table 1 presents the trade-offs between robust and simplified sensing.

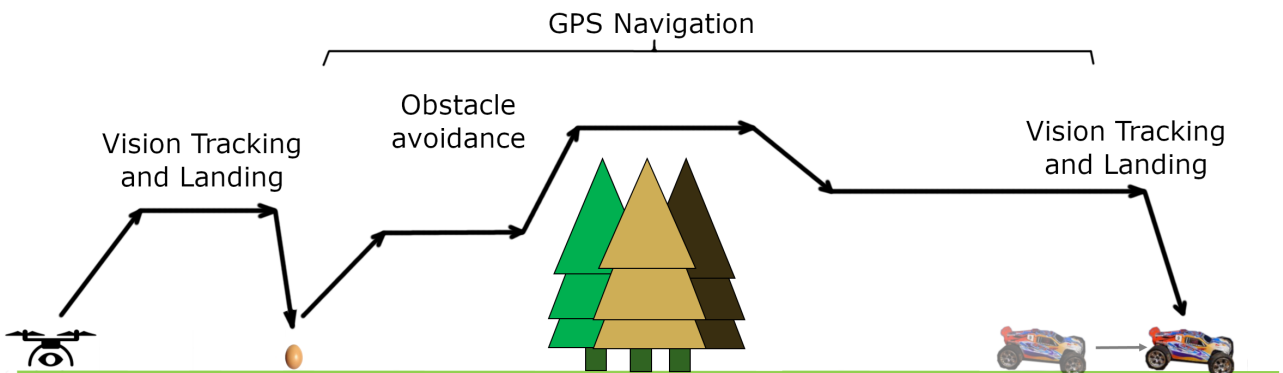


Figure 1: Mission Profile with annotated sensor team challenges

Sensor configuration	Cost	Complexity	Weight
Simple sensor configuration	Low cost, few additional sensors needed	Simple, not original	Low weight
Robust sensor configuration	High cost, requires additional computing power	Complex, prone to incompatibility problems	High weight, requires additional thrust and battery

Table 1: Matrix showing trade-off connected to choosing sensor configuration

2.3 Final choice

For the final setup, a compromise between a robust and simplified sensor configuration was chosen. The robust configuration was too expensive and would require a complete revision of the project as well as initial resources (mainly computing power and thrust). At the same time, the objective was to maximise the sensing possibilities using the already possessed equipment. It was concluded that greater robustness can be achieved using a clever implementation of vision algorithms. Thus, it was decided that the drone will be equipped with the following sensors (Figure 2 presents the sketch of the drone with sensors):

- Wifi adapter to connect with the base station.
- IMU for state estimation (included in RTK GPS and PixHawk controller).
- Here+ RTK GPS for way-point navigation.
- Three Time-Of-Flight TeraRanger sensors pointing forwards for obstacle detection.
- Time-Of-Flight TeraBee 3D camera pointing forwards for obstacle detection.
- One Time-Of-Flight TeraRanger pointing downwards for altitude tracking.
- RGB camera (ELP 2.1 mm lens Webcam) pointing downwards for vision tracking of the package and the landing field.

Due to various incompatibilities and problems, the sensor configuration had to adjust and as a result, had to change throughout the project. This report does not describe the evolution process of every sensor but instead focuses on GPS navigation and specifically RTK GPS: its usage, specification and development throughout the project. Unfortunately, at the beginning of the second test, the RTK GPS stopped functioning correctly and had to be replaced with a conventional positioning device. The next sections present the initially used Here+ RTK GPS as well as the further steps taken after the failure of the RTK GPS.

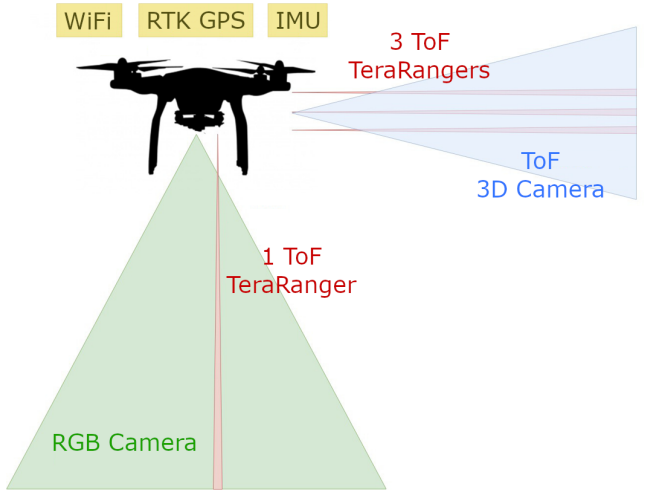


Figure 2: Final sensor configuration

3 GPS Navigation overview

In order to find the delivery point and the landing pad, the drone used GPS navigation. This meant that the drone had to know its own GPS coordinates as well as the coordinates of the landing pad (RC car). The system had to be accurate enough to enable the drone to get the pick-up target as well as the landing pad within the field of view to the downwards pointing RGB camera. For commercial implementation, both the landing pad and the drone could be equipped in high accuracy RTK GPS and the mentioned requirement would easily be achievable. However, for the proof of concept tests, it was decided that the drone's position will be determined using RTK GPS while the RC car will be equipped with a phone which will send its GPS data to the drone via an internet connection. A preliminary analysis determined that with the appropriate algorithm, the landing pad will with high probability fall into the field of view of the camera. The maximisation of the field of view also determined the model of camera - the ELP 2.1 mm lens webcam is a wide angle camera with a 2.1 mm lens [5][6]. The schematic of the GPS navigation system is presented in Figure 3. The mode of work of RTK GPS is presented in the next section.

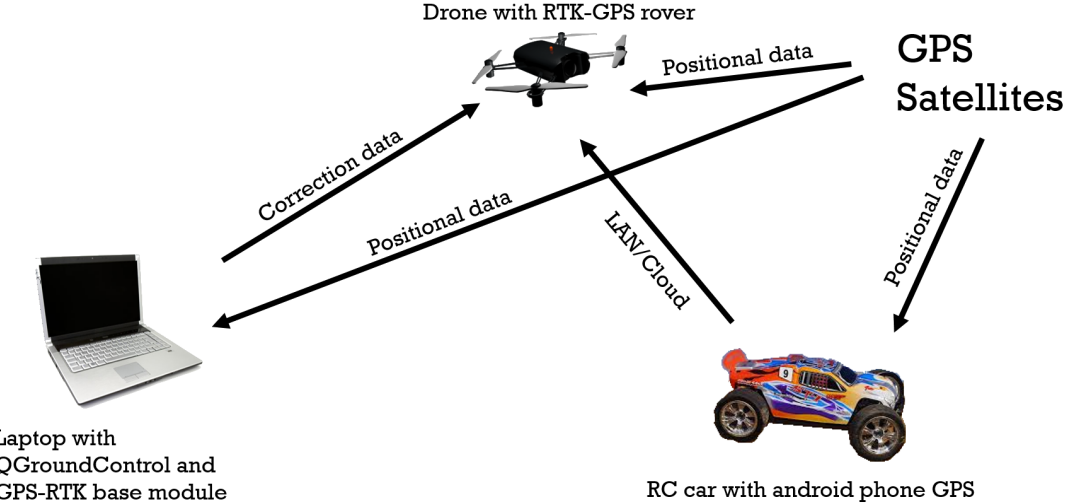


Figure 3: GPS Navigation system schematic

4 Here+ RTK GPS

4.1 Manufacturer specification and usage

Here+ RTK GPS was designed to seamlessly work with QGroundControl software on Linux. The GPS is composed of two parts which both receive GPS data from satellites. The base RTK module (Figure 5), which is connected to a laptop with QGroundControl software (QGC) [7] via a USB cable, and the rover (Figure 6) which is onboard the drone (see Figure 7 for wiring schematic adapted from [8]). The base module is to be kept stationary. Its purpose is to use its own static and very accurate position to correct the GPS positioning of the moving rover. Both the rover and the base are observing the same set of satellites but since the base accurately knows its own position it can sense the positioning errors and can thus make corrections which are then sent to the base rover [9]. Before the base starts to function properly it has to converge on its own position. This can be achieved either by using a survey-in procedure during which the base gathers GPS data over a long period of time (20 minutes to 5 hours depending on desired convergence) or by a manual setup where the user manually sets the coordinates of the base and the accuracy.

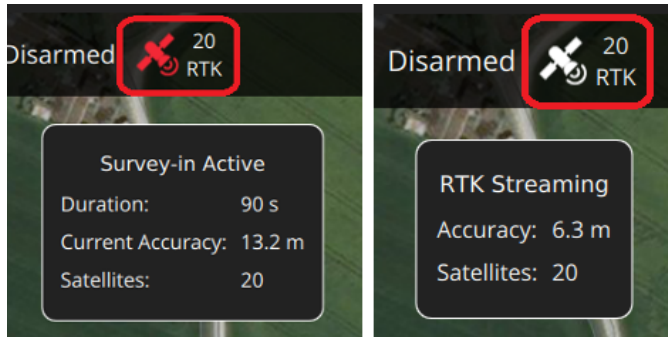


Figure 4: Survey-in status info in QGC (left); RTK GPS streaming status info in QGC (right)

After initial configuration and position convergence, the base starts communicating with the rover through telemetry and the laptop software, sending the correction data in NMEA messages [10]. This enables the rover to establish its position with superior accuracy. The raw GPS data from the rover is automatically processed by the PX4 software installed on the PixHawk controller and it can then be retrieved using Mavros plugin to ROS on ODROID (for more information about ROS and Mavros see [11]).



Figure 5: Base module



Figure 6: GPS rover module

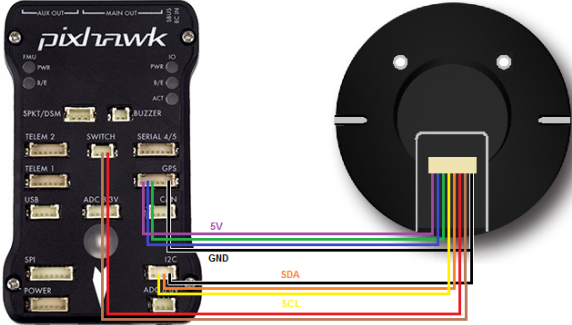


Figure 7: Rover - PixHawk wiring schematic used

The data was transmitted through /mavros/globalposition/ topics:

- /mavros/globalposition/raw/fix - raw GPS coordinates at 5 Hz rate
- /mavros/globalposition/global - GPS coordinates fused with IMU using Kalman Filter at 10 Hz rate

The output from both topics were tested for accuracy and the results are presented in the next sections.

4.2 Mounting the rover on the drone and positioning the base module

For the best performance of both the rover and base, the devices must have a clear view of the sky [8] in order to receive an unblocked signal from the satellites. One thing that can hamper correct functioning of GPS devices is magnetic interference which disturbs the transmitted data as well as influences the compass readings. Source [12] indicates that it can even lead to complete loss of control and critical failure. Documentation in [13] specifies that the rover should be placed high above other onboard equipment in order to minimise the interference from the rotors and radio equipment. As the distance increases, the intensity of magnetic interference decreases. Moreover, to limit the transmission of electromagnetic waves through the frame, the rover was separated from the top of the mast with a 0.5 cm layer of foam. Lastly, following [13] it was ensured that the compass calibration will not be influenced by any nearby metallic items.

It is worth adding that the PX4 autopilot software takes many measures to prevent problems with magnetic interference - the drone does not arm itself if there is too much interference sensed by the magnetometer. If the loss of GPS signal occurs while in flight, warnings are automatically sent to the base station and the flight controller takes predefined fail-safe action e.g. switches to manual control. The above information was reinforced by the example in [14] and by consultations with PhD student Xiao Feng [15]. The resulting position of the GPS rover on the main frame of the drone can be seen in Figure 9.

The GPS base module is, like the rover, a GPS device and thus it should be positioned following the same rules. The manual in [8] specifies that for the optimal performance the base station should be mounted on a tripod far from any electrical devices and ferromagnetic frames. As the tests were carried out in a park the only possible interference was caused by a laptop serving as the base command station. During the first test, the distance from the laptop was about 2 m. After start-up, the base module achieved 1 m accuracy after only 20 minutes.

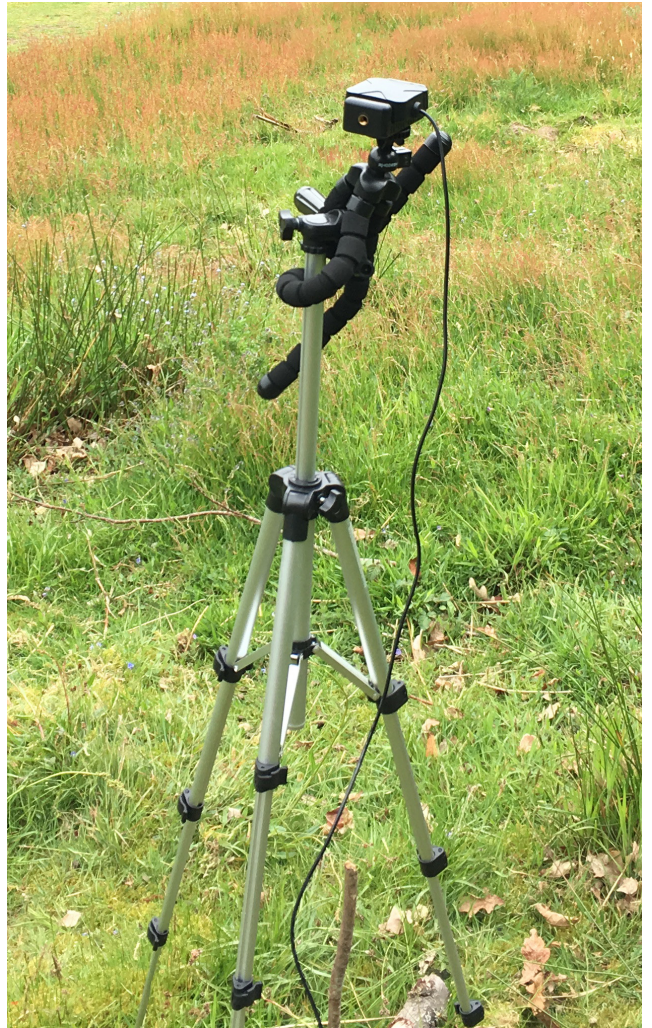


Figure 8: Tripod with base module mounted on top



Figure 9: Drone with GPS rover mounted on the mast

4.3 Accuracy tests

The accuracy of the rover mounted on the drone depends on the converged accuracy of the base module. The tests had been done with a base accuracy of 6 and 2 metres. For both cases, two tests were performed. The testing procedures are presented below.

Test 1 - Static

1. Start the GPS.
2. With the GPS kept stationary record (rosbag) the mavros topics for 3 minutes:
 - /mavros/globalposition/raw/fix
 - /mavros/globalposition/global
3. Convert GPS latlong coordinates to ENU (local Cartesian east-north-up).
4. Plot data.
5. Calculate the mean, noise and random walk.

Test 2 - Circle

1. Start the GPS.
2. With the GPS stationary start recording (rosbag) the mavros topics for 3 minutes:
 - /mavros/globalposition/raw/fix
 - /mavros/globalposition/global
3. Having string attached to the GPS and a stationary pole, walk around the pole three times.
4. Convert GPS latlong coordinates to ENU (local Cartesian east-north-up).
5. Plot data.
6. Calculate the mean radius and deviation.

The results from static tests are presented in Figures 10, 11, 12 and 13. For each test, standard deviations were calculated from the mean position. The drift velocity was calculated by taking measuring average GPS velocity between data points spaced by 2 seconds. For all calculations only /raw/fix data was used but /global data gives almost identical results (within 5%). Papers [16] and [17] indicate that the appropriate way to analyze noise is to use Fourier decomposition. The Fourier decomposition was performed using Matlab. Since the data was sampled at uneven rate with mean of 5 Hz, it was first spline-interpolated using *interp1()* function [18] in order to even-out the sampling points and then a Fourier transform was performed using *fft()* function following the procedure described in [19].

The obtained error amplitude spectra are shown in

Figures 15, 16, 17 and 18. For each accuracy there are two Figures - the first one shows the amplitudes at low frequencies (up to 0.1 Hz) and the other corresponds to higher frequencies (from 0.1 Hz to 4 Hz). This was done to aid the visual examination of the frequency response as the magnitude significantly decreases with frequency. The calculated GPS characteristic quantities from static tests are displayed in Table 2. The results from the circle tests are presented in Figures 20 and 19. For each test, a circle fitting was performed. The fitting procedure is explained below:

1. Single out data points that lie on circle (using visual examination).
2. Determine the probable area for the centre of the best fit circle (using visual examination).
3. Iterating over a discrete domain determined in (2), calculate the distance from all data points and take the average to obtain mean radius.
4. Calculate the mean squared error.
5. Return the circle centre coordinates and mean radius for which the mean squared error is the lowest.

The calculated circle characteristic quantities are displayed in Table 3. The source code of data reduction can be found in Appendix.

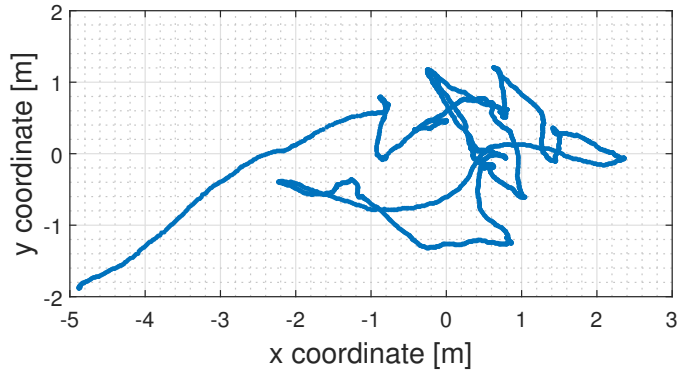


Figure 10: /raw/fix GPS position in ENU frame of reference over time for the base accuracy 6 m

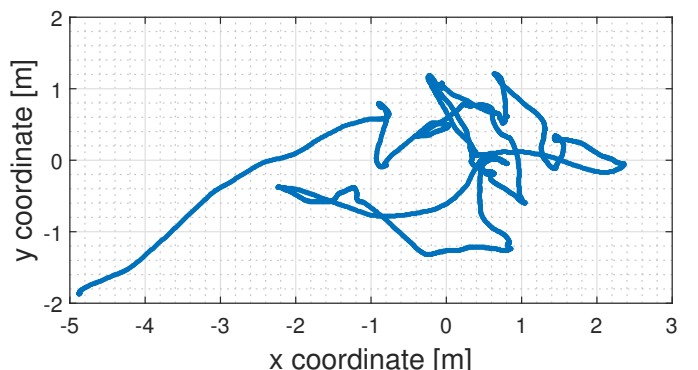


Figure 11: /global GPS position in ENU frame of reference over time for the base accuracy 6 m

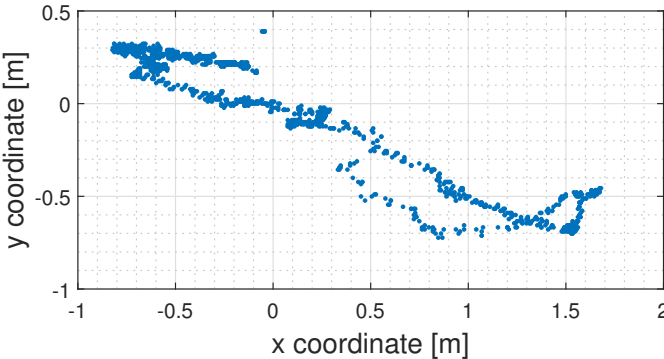


Figure 12: /raw/fix GPS position in ENU frame of reference over time for the base accuracy 2 m

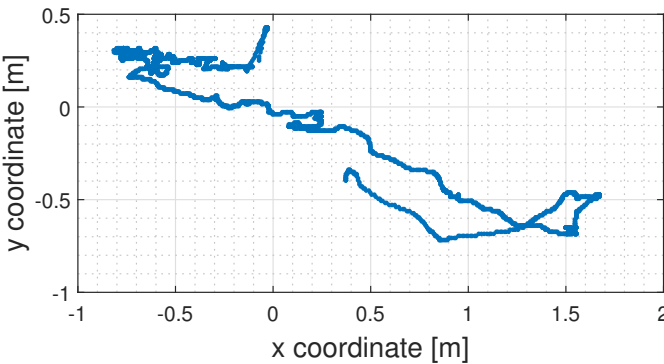


Figure 13: /global GPS position in ENU frame of reference over time for the base accuracy 2 m

4.4 Discussion

4.4.1 Static test accuracy

From Figures 10 to 13 it can be concluded that the GPS readings are very precise relative to their accuracy. Although the rover is held stationary, its GPS position wanders in the proximity with a moderate drift velocity. Examining the results in Table 2, it can be seen that the RTK GPS offers superior accuracy compared to normal GPS Phone. Said accuracy also increases significantly with the accuracy of the base station. The two-dimensional standard deviation is almost two times lower for the base accuracy of 6 m and almost 4 times lower for the accuracy of 2 m. Field testing determined that reaching the base accuracy of 1 m is achievable using a tripod and performing survey-in for about 20 minutes. The relationship between base accuracy and the standard deviation is not proportional but it can be predicted that for 1 m the standard deviation will be about 0.5 m. For the purposes of finding the landing pad, this is sufficient. Most of the limitation stems from the inaccuracy of the Phone GPS mounted on the RC car. As mentioned earlier, the commercial implementation could have both the drone and the landing pad equipped in high accuracy GPS devices meaning that the drone will have no issues in getting within a 1 m radius of the target.

The drift velocity is crucial since it determines the hover movement of the drone. As is the case with standard deviation, RTK GPS offers much greater accuracy compared to Phone GPS. The measured mean drift velocity for the base accuracy of 2 m is 0.02 m/s indicating that the hover movement of the drone is minimal. For the base accuracy of 1 m, it can be forecast that the mean velocity of the signal would be around only 0.01 m/s.

4.4.2 /global vs /raw/fix

As mentioned in the Here+ RTK GPS specification (see Section 4.1), the GPS data was published in two separate ROS topics - one with raw data and one providing data fused with IMU information. The Figures 10 to 13 aid in comparing the differences between the two. For the case with the base accuracy of 6 m, the graphs look almost identical. The graphs for the base accuracy of 2 m provide much more insight. The fusion with IMU data gets rid of the noise from the GPS, preventing the observed position of the GPS rover from making discrete jumps. As a consequence, the /global signal is smoothed out. Nonetheless, the discrete leaps in the /raw/fix topic are very small - of the order 2 cm. The autopilot uses proportional control [20] with data filters and thus it is prepared to cope with this type of noise. For purposes of way-point navigation, the small position jumps do not pose any challenge as it is the big scale accuracy and the calculated long-term standard deviation that is essential.

There was, however, a problem with the /global GPS signal. The circle tests indicated that there can be gaps in the position data as can be seen in Figure 14. All the gaps occur on the left side of the circle which suggests that the phenomenon was caused by the specific location of circle tests. Nonetheless, the lack of GPS data influenced the decision to use /raw/fix data, which, as was earlier demonstrated, is sufficient for the purposes of way-point navigation.

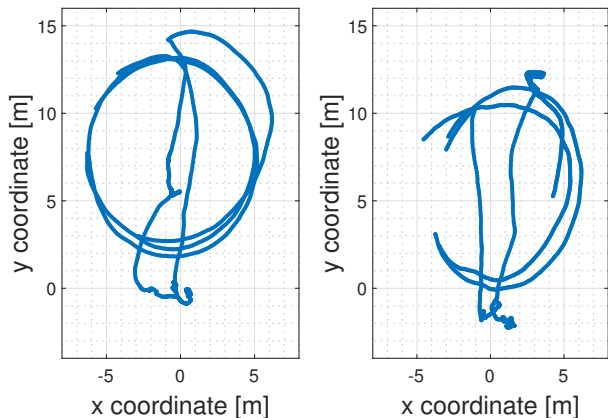


Figure 14: /global GPS data from circle tests with the base accuracy 2 m (left) and 6 m (right)

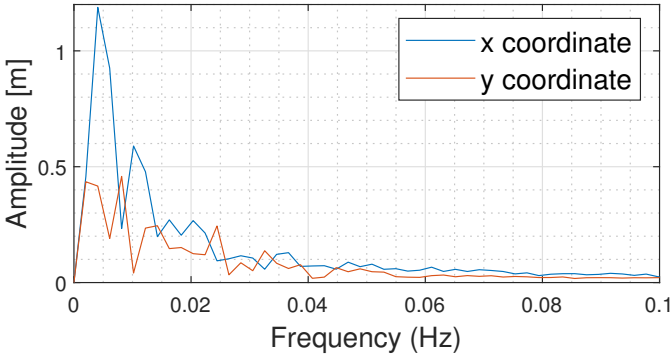


Figure 15: Single-sided amplitude spectrum of GPS coordinates in ENU frame of reference for the base accuracy 6 m for low frequencies $\in (0.0, 0.1)$ Hz

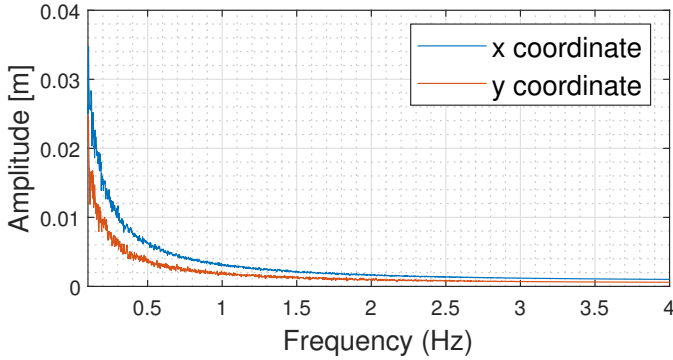


Figure 16: Single-sided amplitude spectrum of GPS coordinates in ENU frame of reference for the base accuracy 6 m for high frequencies $\in (0.1, 4.0)$ Hz

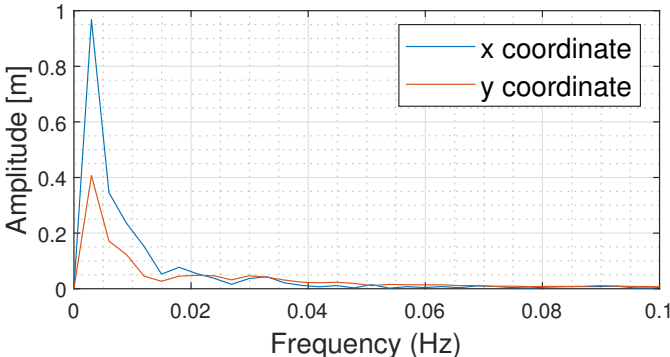


Figure 17: Single-sided amplitude spectrum of GPS coordinates in ENU frame of reference for the base accuracy 6 m for low frequencies $\in (0.0, 0.1)$ Hz

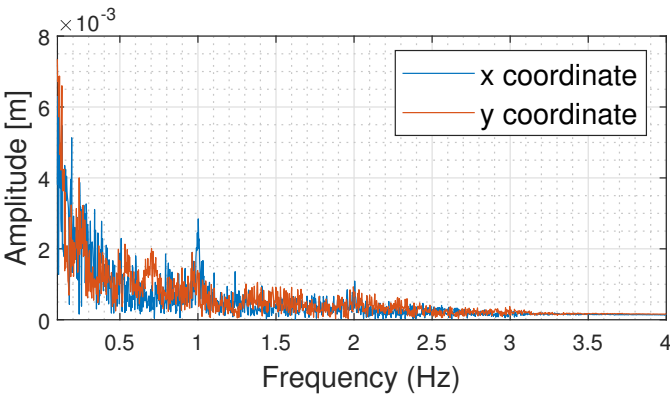


Figure 18: Single-sided amplitude spectrum of GPS coordinates in ENU frame of reference for the base accuracy 2 m for high frequencies $\in (0.1, 4.0)$ Hz

4.4.3 Frequency analysis

Figures 15 to 18 give insight into the amplitude-frequency response of the static GPS signal. The amplitude spectra are in agreement with GPS position vs time graphs in Figures 10 to 13. The most active frequencies are the low frequencies (Figures 15 and 17) with the biggest peak for frequency 0.01 Hz indicating that the global GPS error dynamics have a period of about 100 seconds. The plots look similar qualitatively for both tested base station accuracies, the difference being increased amplitude magnitude for a base accuracy of 6 m by a factor of around 15 %. Furthermore, the amplitude spectrum for the base accuracy of 2 m seems to be more smooth for low frequencies which is most probably caused by the higher accuracy. The "tails" of amplitude-frequency graphs in Figures 16 and 18 provide further information about the small scale noise of the GPS. For the base accuracy of 6 m the variations of frequency higher than 0.1 Hz are smaller than 4 cm and for frequencies higher than 2 Hz they stay below 2 mm. For the base accuracy of 2 m, the amplitude of low scale fluctuations is contained within a millimetre scale.

All of the information contained in the amplitude-frequency graphs provided data about the noise of the GPS devices and was given to the flight control team to enhance the quality of the Gazebo simulations.

Interestingly, it can be concluded from all static test graphs (Figures 10 - 18) and the table with GPS characteristic quantities (Table 2) that the accuracy of the RTK GPS is not isotropic. The accuracy in the y-direction (North-South) is almost twice the accuracy in the x-direction (East-West). This RTK GPS behaviour differs from the Phone GPS behaviour for which the standard deviation in the x-direction is two times smaller than the standard deviation in the y-direction. As the RTK GPS tests were performed in one session and the Phone GPS test was performed on a separate occasion in a different location, this suggests that the error anisotropy is time-dependent and most probably is caused by the momentary position of the GPS satellites or the orientation of the GPS modules. Paper [21] discusses the error directionality and how it can be measured and described. It concludes that proper characterisation of the spatial error requires the usage of circular statics and enough number of checkpoints. For the purposes of the drone navigation, the error anisotropy does not pose a challenge since the standard deviation is still bounded and decreases as the accuracy of the base module is enhanced. The correct analysis could be done for commercial implementation but it would still require significant resources. Usage of RTK GPS significantly diminishes the errors thus reducing a need for a formal and strict analysis.

GPS device	1D Standard deviation from mean in x [m]	1D Standard deviation from mean in y [m]	2D Standard deviation from mean [m]	Mean drift velocity [m/s]	Max drift velocity [m/s]
RTK GPS with base accuracy 2m	0.76	0.34	0.83	0.02	0.13
RTK GPS with base accuracy 6m	1.34	0.69	1.51	0.06	0.20
Phone GPS for reference	1.31	2.60	2.91	0.08	0.65

Table 2: GPS results from static tests (Phone data was obtained using same procedure as with RTK GPS data but at different time and location)

GPS device	Mean radius [m]	Standard deviation of radius [m]
RTK GPS with base accuracy 2m	5.61	0.22
RTK GPS with base accuracy 6m	5.01	0.67

Table 3: GPS results from circle tests

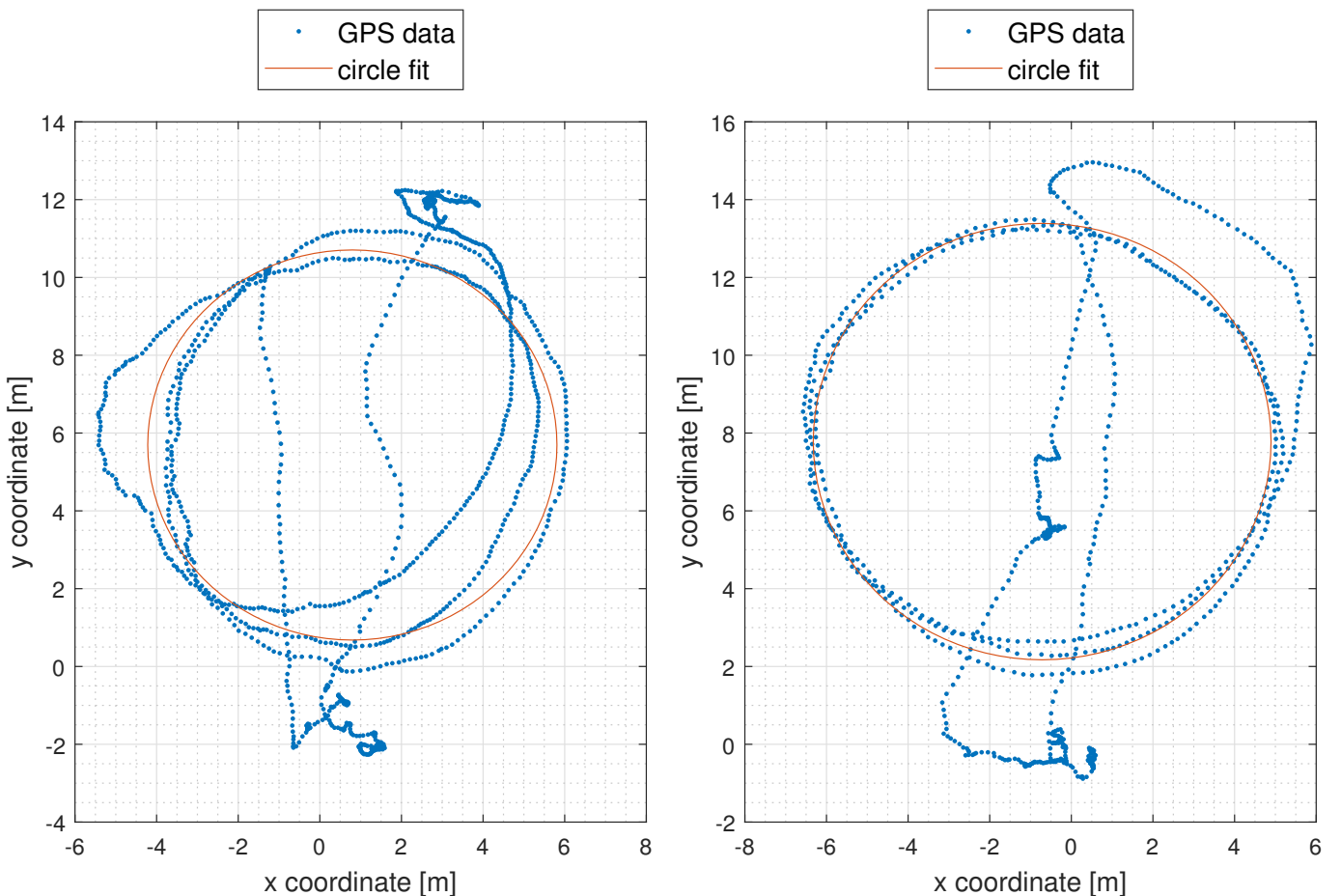


Figure 19: Circle test GPS position in ENU frame of reference over time for the base accuracy of 6m

Figure 20: Circle test GPS position in ENU frame of reference over time for the base accuracy of 2m

4.4.4 Circle tests

Figures 19 and 20 give more insight into the dynamic tracking of the drone. Although the static tests (Figures 10 to 13) indicated fluctuations of magnitude 1 m, the GPS path clearly resembles a circle - ragged for accuracy of 6 m but very precise for the accuracy of 2 m. Looking at the standard deviations in Figure 3 the GPS path is within a quarter of a meter from the ideal circle for base accuracy of 2 m while within a sixth of a meter for a base accuracy of 6 m. For the accuracy of 1 m, we could expect stand deviation to be around 0.1 m. This is important from the point of view of obstacle avoidance. The drone might not perfectly know its position but if it encounters an obstacle, its relative position will not dramatically change as to impede the correct, programmed behaviour and the obstacle will be avoided successfully.

Furthermore, the graphs indicate that there is no positioning anisotropy and the GPS correctly tracks the spatial movement. The GPS anisotropy affects only the positioning error. To reinforce this observation, the histograms of radius deviation have been plotted in Figures 21 and 22. Clearly, the distributions can be classified as normal random process distribution. If there was a problem with spatial positioning anisotropy the graph would show more than one peak in radius distributions.

4.5 Improving GPS performance with HxGN SmartNet

Although the Here+ RTK GPS uses its own base module for position correction it is not the requirement to use this specific base or use only one base. Hexagon company offers HxGN SmartNet service which enables GPS devices to correct their position using a network of specialised, stationary bases [1]. One of the bases is shown in Figure 23.

Unfortunately, Hexagon company does not offer the possibility of short term testing. The cheapest package which offered some access to the network cost £489.25 [1] which was too expensive for the project budget. Nonetheless, the prices do not depend on the

number of devices being connected to the network. Thus, for the commercial implementation, the price of using the network per device would decrease with the number of drones being used in the field.

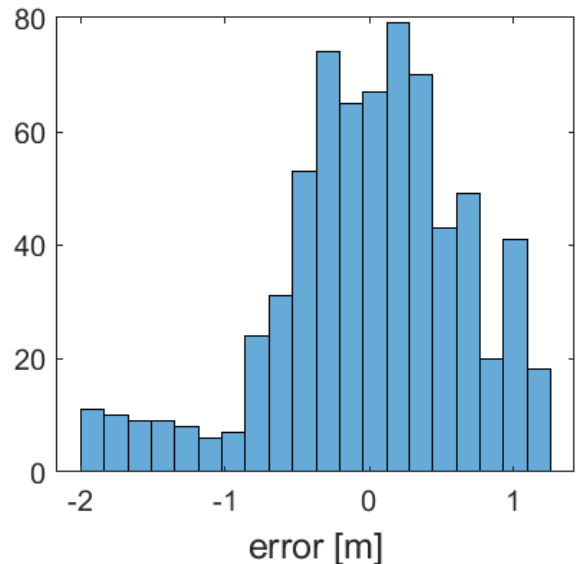


Figure 21: Radius error distribution for base accuracy 6 m

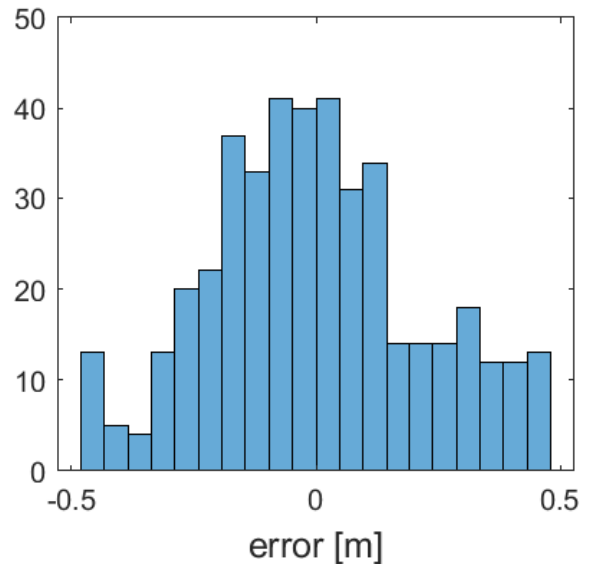


Figure 22: Radius error distribution for base accuracy 2 m



Figure 23: HxGN SmartNet base station (adapted from [1])

5 RTK GPS failure

During the setup of the second test in Silwood, the base module of the Here+ RTK GPS stopped to correctly perform survey-in. The base position accuracy was stuck at 94868.3 m (see Figure 24). At first, it was determined that the probable reason could be detached wires (see Figure 24) as the cable end was in a bad condition.

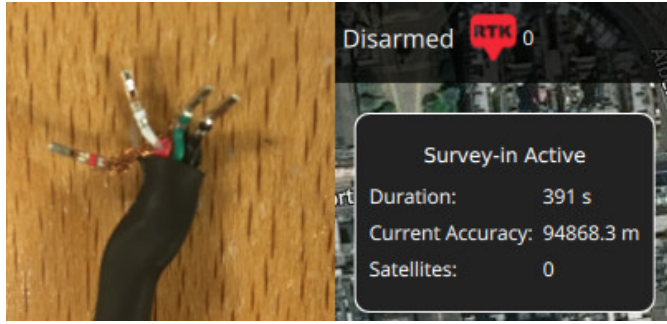


Figure 24: Base module cable end (left) and the survey-in status information indicating the problem (right)

However, after soldering and checking that the connections work, the base response was identical. After consultations [15], it was determined that the problem could stem from the firmware problem. Both the base module and the rover were rebooted and new firmware was loaded. Unfortunately, this has also failed to fix the wrong behaviour of the base module. It was responding in the same way as when the problem had initially occurred. The issue was reported to the manufacturer of the Here+ RTK GPS - Hex Technology Limited. The company has acknowledged the incident and pointed to some troubleshooting options [22]. Firstly, it was made sure that the problem is not due to software problems. Here+ RTK GPS is specifically designed to work on Windows with Mission Planner as well as the manufacturer software U-Center [8]. This option was tried out but gave the same results. The next instruction obtained from the Hex Technology representative was to use the U-Center and to repeatedly change the setup method from survey-in to manual coordinate setup. U-Center allows to strictly monitor the messages coming from and to the base module. Although the proposed procedure did not fix the base, the RTK GPS messages were recorded and sent to the Hex Technology. After examining the recorded files, the Hex Technology representative concluded that there is a configuration problem that the U-Blox chip is stuck in. Thus the instruction was to do the same procedure as earlier but this time also record log files which could then be examined in detail by the U-Blox engineers. U-Blox is a company that provides the chip which is used by Here+ RTK GPS. As of this moment, this is still being done and thus the RTK GPS was not available for testing.

5.1 Substitution evaluation

5.1.1 Manual base coordinates setup

RTK GPS offers the possibility to manually set up the coordinates of the base module. Tests with the QGroundControl determined that it is possible and the base starts to stream data to the rover. However, the preliminary analysis indicated that the accuracy is not being corrected as the GPS position wandered in the area of radius 6 m, which is similar to conventional Phone GPS. This was supported by the observation that the base module does not recognise any satellites. Without the feedback from satellites, it is not possible for the base to send valid correction data [9].

5.1.2 RTK GPS Reach

The Aerial Robotics Lab which is supporting the project offered the substitution for Here+ RTK GPS - the RTK GPS Reach. The new device reportedly has lower accuracy but also performs well as it employs the RTK technology [15]. The RTK GPS Reach has a better user interface as each of the modules (the base and the rover) can be used interchangeably and each of them is actually a small computer with which a user communicated via WiFi connection using a browser application [23]. The GPS was successfully set up, however, it was revealed that the device does not support communication with PX4 autopilot software. As a result, the PixHawk cannot use the Reach RTK GPS for state estimation and is not able to arm itself for flight. One solution could be to use two GPS devices. One conventional GPS which would serve the PixHawk for state estimation and the RTK GPS Reach which would communicate with PixHawk via ROS on the ODROID computer. This solution was discarded as it would be too time-consuming to write software for GPS - ODROID communication that would be able to successfully and efficiently offer increased accuracy. Furthermore, this solution would be only a temporary replacement for RTK GPS and thus not essential for purposes of proof-of-concept testing.

6 Final solution

Due to limited options, the final decision was to use just the rover of the Here+ RTK GPS meaning that it will not receive any correction data and its precision should be comparable to a normal GPS. The same tests that were performed for RTK GPS were performed for just the rover. The results are presented in Figures 25, 26 and 27 as well as Table 4. Figure 25 shows the static path of the GPS signal, Figures 26 and 27 show the amplitude frequency response similarly to Figures 15 - 18. Table 4 provides the GPS characteristics - the same as the ones presented in Table 2 but in this case for the RTK GPS rover.

GPS device	1D Standard deviation from mean in x [m]	1D Standard deviation from mean in y [m]	2D Standard deviation from mean [m]	Mean drift velocity [m/s]	Max drift velocity [m/s]
RTK GPS rover without the base	0.50	0.66	0.83	0.05	0.35

Table 4: GPS results from static test on the rover without the base corrections

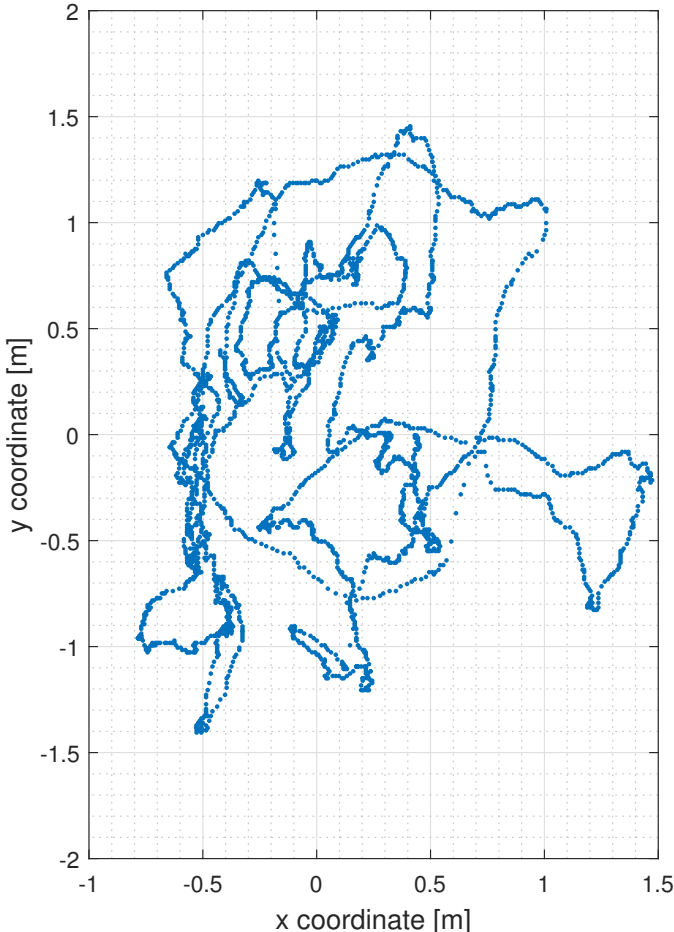


Figure 25: /raw/fix GPS position in ENU frame of reference over time for the rover without the base corrections

6.1 New accuracy discussion

Comparing the new results with results in Section 4.4 it can be concluded that the accuracy of the rover is relatively good with 2D standard deviation being the same as for the static test with the base accuracy of 2 m. Moreover, the anisotropy of measurements is reduced as the difference between standard deviations in x and y is smaller. This reinforces the earlier conclusion that the momentary accuracy of the GPS devices is not constant with time but can change quite dramatically in the long term. It is important however to note that the standard deviation does not encompass every information about the accuracy of the GPS. Comparing Figure 12 for the base accuracy 2 m with Figure 25 for just the rover it can be inferred that although the standard deviation is the same, all of the readings for the base accuracy of

2 m are contained inside 1.5x3 m rectangle while the rover readings spread over a rectangle with dimensions 2.5x3 m. The characteristics of the drift speed of the rover from the static test are also similar to the ones obtained with a working base module. The mean drift speed value is in the same regime as with the base and although the maximum drift speed is increased, it is still lower than for the Phone GPS. The amplitude - frequency graphs in Figures 26 and 27 confirm the reached conclusions. The accuracy of the rover results fits in between the accuracy with the base position precision of 2 m and the base position precision of 6 m. Furthermore, the amplitudes in x- and y-directions are much closer to each other which contributes to the decreased positioning error.

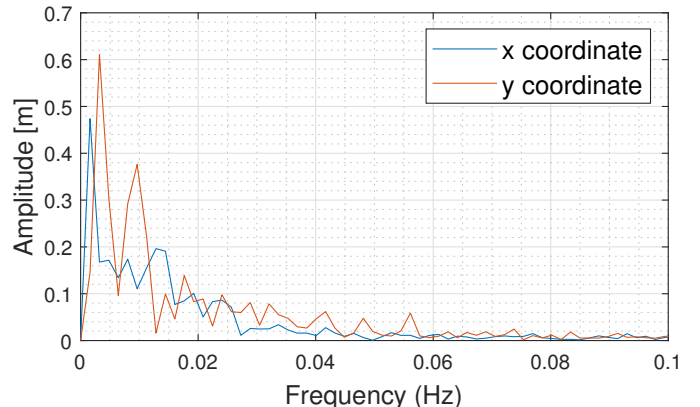


Figure 26: Single-sided amplitude spectrum of GPS coordinates in ENU frame of reference for the rover without base corrections for low frequencies $\in (0.0, 0.1)$ Hz

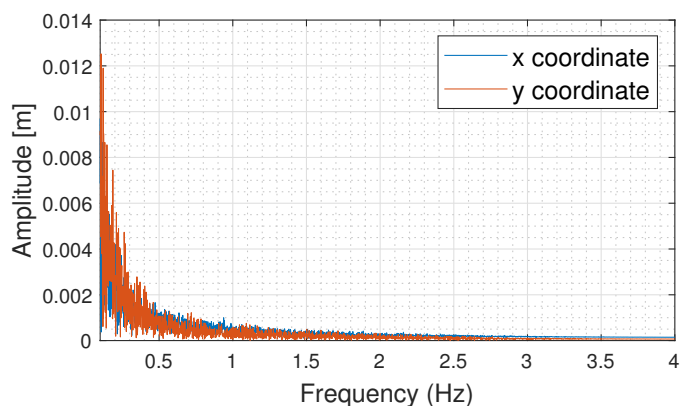


Figure 27: Single-sided amplitude spectrum of GPS coordinates in ENU frame of reference for the rover without base corrections for high frequencies $\in (0.1, 4)$ Hz

Furthermore, the consultations with the student responsible for the Phone GPS revealed that the standard deviation of the noise for the Phone GPS can also significantly vary with time - sometimes being as low as 1 m and sometimes reaching 4 m. This reinforces the previously reached conclusion that the accuracy of the rover is time and conditions dependent, indicating that the exceptional accuracy of the rover might be incidental.

6.2 Performance at Silwood testing site (Figure 28)

The tests at Silwood showed that the drone was not able to fully perform its mission profile. The drone could still fly, hover and complete some of the tasks but all the separate challenges could not be fitted together into a single flight. This was not caused by a single error - many things contributed to final imperfect performance which eventually resulted in the crashing of the drone and destruction of the pick-up mechanism.

The GPS rover worked as the drone could arm itself and hover. Furthermore, it successfully performed way-point navigation and managed to reach the RC car with Phone GPS.

Nonetheless, the rover was significantly drifting away. It is not trivial to say what was the source of this behaviour. On one hand, as the static tests indicate, the drift speed of the rover is quite significant. However, according to the testing group [24], it was really windy on the day. Thus it might be that the incorrect performance was caused by the fact that the drone could not efficiently withstand the adverse conditions. Nevertheless, it is certain that using the rover without the base corrections was hindering the correct behaviour of the vehicle. Having the working base module with its position accuracy converged to 1 m would definitely improve the performance throughout the tests.



Figure 28: Testing site at Silwood

7 Conclusions

1. RTK GPS is a robust device that offers superb positioning accuracy. The performance highly depends on the position convergence of the base module. Having the base module converge to the accuracy of 1 m would enable the drone to precisely determine its position improving both its controllability and performance of the required mission profile. The drone will be able to get into close proximity of the egg and the landing pad which will then enable vision tracking of the landing and respectively pick-up of the egg and landing in the final destination.
2. The main source of limitations is the positioning accuracy which depends on the location and the conditions (robustness of used GPS device, availability of GPS signal and weather).
3. The accuracy tests determined that although the long term position will vary with quite a significant standard deviation relative to the size of the drone, the mean drift speeds are quite low and the drone will not take any dramatic movements in order to keep a constant GPS position.
4. There is specific anisotropy of GPS signal error which changes with time as well as the orientation of the GPS device. Although it influences the overall error, it does not pose a significant problem as the accuracy is still being bounded by the base station degree of convergence.
5. The frequency analysis determined that most of the error comes from slow fluctuations of period approximately 100 seconds. The signal also contains momentary white noise but it is very small in magnitude and can be easily eliminated using the data from the IMU.
6. The RTK GPS rover which does not receive corrections from the base module can still be an accurate positioning device and can offer very good precision as long as the location and weather conditions are favourable. Therefore, the usage of conventional GPS does not greatly impede the performance of the mission profile. The drone can still successfully use it for state estimation and performance of simplified objectives.
7. The large scale implementation offers improvements in the performance of the RTK GPS. The drones would have access to a larger set of bases which would further increase the positioning accuracy and facilitate the performance of the objectives.

References

- [1] HxGN SmartNet. <https://hxgnsmartnet.com/en-gb>. Accessed: 2019-06-11.
- [2] J. Thomas, J. Welde, G. Loianno, K. Daniilidis, and V. Kumar. Autonomous flight for detection, localization, and tracking of moving targets with a small quadrotor. *IEEE Robotics and Automation Letters*, 2(3):1762–1769, July 2017.
- [3] J. Kim, Y. Jung, D. Lee, and D. H. Shim. Outdoor autonomous landing on a moving platform for quadrotors using an omnidirectional camera. In *2014 International Conference on Unmanned Aircraft Systems (ICUAS)*, pages 1243–1252, May 2014.
- [4] Abraham Bachrach, Samuel Prentice, Ruijie He, and Nicholas Roy. RANGE-Robust autonomous navigation in GPS-denied environments. *Journal of field robotics.*, 28(5):644–666, 2011.
- [5] Amazon description of "ELP 2.1 mm lens Webcam Windows Linux 720P Wide Angle USB Camera Module". <https://www.amazon.co.uk/ELP-Webcam-Windows-Camera-Module/dp/B01C2PIBBO>. Accessed: 2019-05-17.
- [6] ELP 1MP AUDIO USB CAMERAS, H.264. http://www.webcamerausb.com/1mp-audio-usb-cameras-h264-c-37_43/. Accessed: 2019-06-12.
- [7] QGroundControl homepage. <http://qgroundcontrol.com/>. Accessed: 2019-06-08.
- [8] Here+ RTK GPS. <http://ardupilot.org/copter/docs/common-here-plus-gps.html>. Accessed: 2019-06-12.
- [9] Lambert Wanninger. Introduction to Network RTK. <http://www.wasoft.de/e/iagwg451/intro/introduction.html>, 16 June 2008. Accessed: 2019-06-12.
- [10] NMEA data. <https://www.gpsinformation.org/dale/nmea.htm>. Accessed: 2019-06-12.
- [11] ROS Wiki. <http://wiki.ros.org>. Accessed: 2019-05-26.
- [12] Johnatan Feist. Does your drone need GPS? <https://www.dronerush.com/drone-gps-10778/>, 2 May 2019. Accessed: 2019-05-22.
- [13] Magnetic interference - ardupilot rover documentation. <http://ardupilot.org/rover/docs/common-magnetic-interference.html>. Accessed: 2019-05-22.
- [14] DJI Flame Wheel 450 with Distance Sensor and RTK GPS (Pixhawk 3 Pro). https://docs.px4.io/en/frames_multicopter/dji_flamewheel_450.html. Accessed: 2019-05-23.
- [15] Consultation with PhD student Xiao Feng. May, June 2019.
- [16] Ksenia Dmitrieva. Noise in GPS time series: The contribution of random walk noise. In *SCEC community geodetic model workshop*. Stanford University, 31 May 2013.
- [17] Ivan Rumora, Nenad Sikirica, and Renato Filjar. An experimental identification of multipath effect in GPS positioning error. *TransNav: International Journal on Marine Navigation and Safety of Sea Transportation*, 12, 2018.
- [18] 1-D data interpolation function interp1() reference. <https://uk.mathworks.com/help/matlab/ref/interp1.html>. Accessed: 2019-06-02.
- [19] Fast Fourier Transform function fft() reference. <https://uk.mathworks.com/help/matlab/ref/fft.html>. Accessed: 2019-06-02.
- [20] Multicopter PID Tuning Guide. https://docs.px4.io/en/config_mc/pid_tuning_guide_multicopter.html. Accessed: 2019-06-12.
- [21] Angel Felicísimo, Aurora Cuartero, and María-Eugenio Polo. Analysis of homogeneity and isotropy of spatial uncertainty by means of GPS kinematic check lines and circular statistics. 07 2006.

- [22] Private email conversation with Hex Technology Limited representative. June 2019.
- [23] Emlid M+ docs. <https://docs.emlid.com/reachm-plus/quickstart/>. Accessed: 2019-06-08.
- [24] Private conversation with team member Gerald Bi Low. June 2019.

A Appendix

The code for the data reduction as well as the raw data can be found in Github repository at:
https://github.com/gdp-drone/GDP_GPS_code